# Dynamics of nanoscale ripple relaxation on alloy surfaces

Ashwin Ramasubramaniam*
*Program in Applied and Computational Mathematics, Princeton University, Princeton, New Jersey 08544, USA*

Vivek B. Shenoy†
*Division of Engineering, Brown University, Providence, Rhode Island 02912, USA*

(Received 3 October 2007; revised manuscript received 8 December 2007; published 14 February 2008)

As an alloy surface evolves under capillary forces, differing mobilities of the individual components can lead to kinetic alloy decomposition at the surface. In this paper, we address the relaxation of nanoscale sinusoidal ripples on alloy surfaces by considering the effects of both *surface* and *bulk* diffusion. In the absence of bulk diffusion, we derive exact analytical expressions for relaxation rates and identify two natural time scales that govern the relaxation dynamics. Bulk diffusion is shown to reduce kinetic surface segregation and enhance relaxation rates, owing to intermixing near the surface. Our results provide a quantitative framework for the interpretation of relaxation experiments on alloy surfaces.

DOI: 10.1103/PhysRevE.77.021601 PACS number(s): 81.15.Aa, 68.35.Fx, 68.35.Md

## I. INTRODUCTION

Morphological evolution of crystalline surfaces has been the focus of many theoretical and experimental studies since the early work of Herring [1] and Mullins [2]. Their theories have provided the basis for the determination of surface kinetic parameters, for example, by experimental measurements of the relaxation rates of simple shapes such as sinusoidal ripples [3,4]. Nanoscale technology has spurred renewed interest in this problem since small feature sizes amplify surface effects thereby influencing the stability and performance of nanoscale devices. Many applications require the use of heterostructures or alloys where the surface shape evolution is strongly coupled to compositional variations in the bulk and at the surface. Unlike the case of single component surfaces, where classic solutions are available for shape evolution via surface diffusion, very few analytical solutions are available for surface dynamics in alloy systems even for fundamental problems such as the relaxation of a periodic surface ripple. The only significant theoretical work along these lines for alloy systems is that of Tersoff [5], who provided a numerical solution for the classic Mullins problem [2] by focusing attention on the very early stages of relaxation by surface diffusion.

In the present work, we consider smoothing of sinusoidal ripples in the context of alloy films and provide *analytical* expressions for the relaxation time in terms of the thermodynamic and kinetic parameters. We are particularly interested in the relaxation of nanoscale ripples, which clearly show strong coupling between composition and surface evolution; the model itself does not have an inherent length scale and is generally applicable to any surface modulation. In Sec. III, we demonstrate that in the absence of bulk diffusion there are two natural time scales for relaxation that are typically well separated in magnitude. As a result of this clear separation of scales, the longer time scale effectively determines the overall relaxation of the profile, the shorter time scale only being of consequence during initial transients. In Sec. IV, we include the effects of bulk diffusion and show that when the interdiffusion constant is within a couple of orders of magnitude of surface diffusion constants, intermixing near the surface is very effective in suppressing decomposition induced by the difference in surface diffusivities of the alloy components. Consequently, surface relaxation is able to proceed at an enhanced rate. Our analytical results can be used to readily determine surface and bulk diffusion constants from experimental measurements of surface relaxation.

## II. MODEL FOR RELAXATION OF ALLOY SURFACES

Consider an alloy film represented by the half-space $-\infty < x < \infty$, $-\infty < y \leq 0$. The alloy consists of two atomic species $A$ and $B$ with compositions $c_b$ and $1-c_b$, respectively. We assume throughout this work that the alloy is thermodynamically stable against phase separation, so that composition inhomogeneities come solely from differences of diffusivities. Our goal is to describe the evolution of a modulation on the surface $y=0$ of this alloy film.

Mass transport on the surface is driven by two separate contributions, the first arising from concentration gradients (described by Fick's law) and the second arising from capillarity [1,2]. Assuming terrace diffusion limited kinetics on the surface, the surface mass current of species $i$, denoted by $\mathbf{j}_i$, may then be expressed as

$$\mathbf{j}_i = -D_i \rho_s \nabla_s c_{s,i} + \frac{D_i \Omega \rho_s c_{s,i} \gamma}{k_B T} \nabla_s \kappa. \tag{1}$$

The first term in this expression smoothens out composition gradients at the surface while the second term smoothens out any surface undulations (minimizes capillary forces). In the above expression, $D_i$, the surface diffusion constant of species $i$, $\rho_s$, the areal density of mobile adspecies, and $\Omega$, the atomic volume, are all material-specific parameters. While the surface energy $\gamma$ is, in general, a function of both the orientation of the surface as well as the local composition, to

*aramasub@princeton.edu
†Vivek_Shenoy@brown.edu

 

bring out the essential features of kinetic segregation while keeping the model analytically tractable, we will assume throughout this work that the surface energy is independent of both orientation and composition. Thus, $\gamma$ is also a material-specific parameter. Similarly, for analytical convenience the atomic volumes of the two species are assumed to be identical. The height of the surface $h$, the surface curvature $\kappa=\nabla_s^2 h$, $\nabla_s$ being the surface gradient operator, and the surface composition $c_{s,i}$, of species $i$, vary spatially and in time. We assume negligible vacancy concentration at the surface so that $c_{s,A}+c_{s,B}=1$. From here on, we simplify notation by using $c_s$ to denote the composition of species $A$ at the surface, the composition of $B$ then being $1-c_s$. Conservation of mass allows us to relate changes in surface shape to the mass fluxes $\nabla_s \cdot \mathbf{j}_i$, as

$$v_n = -\Omega \nabla_s \cdot (\mathbf{j}_A + \mathbf{j}_B), \tag{2}$$

where $v_n$ is the normal velocity of the surface.

To close the above set of equations, we specify evolution equations for the composition. First consider the case where surface diffusion is the sole mode of mass transport. Since the alloy is thermodynamically stable against phase separation, the evolution of surface composition is driven entirely by deviations of the ratio of mass fluxes $\nabla_s \cdot \mathbf{j}_A / \nabla_s \cdot \mathbf{j}_B$ from the stoichiometric ratio $c_\Gamma/(1-c_\Gamma)$, as

$$\delta_s \frac{\partial c_s}{\partial t} = \Omega[(c_\Gamma - 1)\nabla_s \cdot \mathbf{j}_A + c_\Gamma \nabla_s \cdot \mathbf{j}_B], \tag{3}$$

where $\delta_s$ is the thickness of the surface layer and $c_\Gamma$ is the composition of the material immediately below the surface layer. Appendix A provides a detailed derivation of this result. In general though, the composition at the surface can also be altered via mass exchange with the underlying bulk. The above expression for surface composition evolution can be generalized to include this additional mechanism as

$$\delta_s \frac{\partial c_s}{\partial t} = \Omega[(c_\Gamma - 1)\nabla_s \cdot \mathbf{j}_A + c_\Gamma \nabla_s \cdot \mathbf{j}_B] - D_b \left.\frac{\partial c}{\partial n}\right|_\Gamma, \tag{4}$$

where the last term represents the flux of atoms arriving at the surface due to interdiffusion from the underlying bulk, $D_b$ being the interdiffusion constant and $\mathbf{n}$ being the unit normal at the bulk-surface interface $\Gamma$. Finally, composition evolution in the bulk is described by the standard diffusion equation as

$$\frac{\partial c}{\partial t} = D_b \left(\frac{\partial^2}{\partial x^2} + \frac{\partial^2}{\partial y^2}\right) c. \tag{5}$$

Equations (1), (2), (4), and (5) are the governing equations of our model describing surface relaxation in alloy films. Of these, Eqs. (1), (2), and (4) describe the evolution of surface height and composition while Eq. (5) describes composition evolution in the bulk. The coupling between surface and bulk fields occurs directly through the last term in Eq. (4) (interdiffusion flux) and indirectly through boundary conditions as will be discussed later in Sec. IV. The limiting form of these equations in the case of vanishing bulk diffusivity has been considered in previous work [5–7].

Although the above governing equations (1), (2), (4), and (5) are nonlinear, in the spirit of Mullins' work [2], we pursue a solution for small perturbations in height and composition, i.e., $|\nabla_s h| \ll 1$ and $(c-c_b) \equiv \zeta \ll 1$, respectively. The governing equations to linear order (derived in Appendix B) are

$$\frac{\partial h}{\partial t} = A_1 \frac{\partial^2 \zeta_s}{\partial x^2} - B_1 \frac{\partial^4 h}{\partial x^4}, \tag{6a}$$

$$\frac{\partial \zeta_s}{\partial t} = A_2 \frac{\partial^2 \zeta_s}{\partial x^2} - B_2 \frac{\partial^4 h}{\partial x^4} - \frac{D_b}{\delta_s} \left.\frac{\partial \zeta}{\partial y}\right|_{y=0}, \tag{6b}$$

$$\frac{\partial \zeta}{\partial t} = D_b \left(\frac{\partial^2}{\partial x^2} + \frac{\partial^2}{\partial y^2}\right) \zeta, \tag{6c}$$

where $\zeta_s \equiv \zeta(x,0,t)$. We assume henceforth that species $B$ is the slower of the two species, so that $0 < D_B < D_A$. The coefficients in the linearized equations

$$A_1 = \Omega \rho_s (D_A - D_B),$$

$$A_2 = \Omega \rho_s \frac{D_A(1-c_b) + D_B c_b}{\delta_s},$$

$$B_1 = \frac{\Omega^2 \rho_s \gamma}{k_B T}[D_A c_b + D_B(1-c_b)],$$

$$B_2 = \frac{\Omega^2 \rho_s \gamma}{k_B T} \frac{c_b(1-c_b)(D_A - D_B)}{\delta_s},$$

are then all positive. Analytical solutions for relaxation by surface diffusion will be presented in Sec. III and those for combined surface and bulk diffusion will be presented in Sec. IV.

Before concluding this section, a few comments about the model are pertinent. As noted previously, the surface energy is assumed to be independent of orientation in this work. Furthermore, we also assume that the surface energy is independent of composition and do not consider surface segregation effects. Then, for near-equilibrium situations such as surface relaxation (this work and [5]) or the growth of elastic instabilities [6], the surface composition $c_s(x,t)$ is just the limiting value of the bulk composition $c(x,y,t)$ at the surface. However, in nonequilibrium situations, even in the absence of a thermodynamic driving force for segregation, purely kinetic effects can lead to the surface composition being different from the bulk as demonstrated by Shenoy *et al.*'s work [7] on sputtering of alloy surfaces. It should also be noted that the film-vacuum interface is treated as a uniform layer of thickness $\delta_s$, the surface composition $c_s$ being an average across this layer. This simple model for the surface layer, while adequate for the present, will require modification in the event that the alloy surface is thermodynamically unstable and forms surface domains.

## III. RELAXATION BY SURFACE DIFFUSION

First consider the situation where surface diffusion is the sole transport mechanism ($D_b=0$) in which case, Eqs. (6a)

TABLE I. Parameters used in numerical calculations. Material constants $\Omega$ and $\gamma$ are representative of sputter ripples on Si(001) [7].

| $\gamma$ | $\Omega$ | $\delta_s$ | $k_BT$ | $\lambda$ | $h_0$ | $L=\Omega\gamma/k_BT$ |
|---|---|---|---|---|---|---|
| 1 J/m$^2$ | 0.02 nm$^3$ | 0.5 nm | 75 meV | 50 nm | 5 nm | 1.7 nm |

and (6b) completely describe the dynamics. Representing the height and composition variations as $[h,\zeta_s]\equiv[\bar{h},\bar{\zeta}_s]e^{ikx-\omega t}$, where $k=2\pi/\lambda$ is the wave number, we obtain from Eqs. (6a) and (6b) a characteristic equation that gives two relaxation rates

$$\omega_{1,2}=\frac{k^2}{2}[(A_2+B_1k^2)\pm\sqrt{(A_2-B_1k^2)^2+4A_1B_2k^2}]. \quad (7)$$

This seemingly complicated expression for the relaxation rates can be shown to have an elegant interpretation as follows. First, recall that the classical result for the relaxation rate of a single component system [2] is

$$\omega=\frac{\Omega^2\rho_s\gamma}{k_BT}Dk^4. \quad (8)$$

This expression furnishes a direct means of extracting the surface diffusivity $D$ from an experimental measurement of the relaxation of a modulation. Next, note that to leading order in the wave number, the relaxation rates $\omega_{1,2}$ for the two-component system may be written as

$$\omega_1=\Omega\rho_s\frac{D_A(1-c_b)+D_Bc_b}{\delta_s}k^2+O(k^4), \quad (9a)$$

$$\omega_2=\frac{\Omega^2\rho_s\gamma}{k_BT}\frac{D_AD_B}{D_A(1-c_b)+D_Bc_b}k^4+O(k^6). \quad (9b)$$

By comparing Eqs. (8) and (9) it is immediately apparent that the relaxation of a two-component modulation is controlled by two *effective* diffusivities

$$D_1^{\text{eff}}=\frac{1}{k^2}\frac{k_BT}{\Omega\gamma\delta_s}[D_A(1-c_b)+D_Bc_b] \quad (\text{from } \omega_1), \quad (10a)$$

$$D_2^{\text{eff}}=\frac{D_AD_B}{D_A(1-c_b)+D_Bc_b} \quad (\text{from } \omega_2), \quad (10b)$$

the latter, in particular, being the *composition-weighted* harmonic mean of the diffusivities of the individual species. Furthermore, the ratio of the relaxation rates is

$$\frac{\omega_1}{\omega_2}=\frac{D_1^{\text{eff}}}{D_2^{\text{eff}}}\propto\frac{D_A}{D_B}\frac{\lambda^2k_BT}{\Omega\gamma\delta_s}.$$

Since the thickness of the surface layer $\delta_s$ and the quantity $L\equiv\Omega\gamma/k_BT$, which has dimensions of length, are typically of the order of a few atomic spacings (refer to Table I), $\omega_1$ is larger than $\omega_2$ by a few orders of magnitude, even for nanoscale modulations; if $D_B\ll D_A$ the difference is further magnified. Therefore, $\omega_1$ should determine fast transients, typically at the early stages of surface evolution, whereas "true" relaxation is controlled by $\omega_2$.

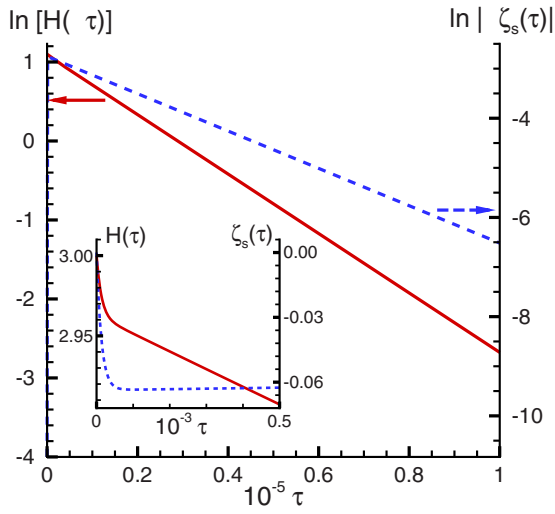


FIG. 1. (Color online) Evolution of modulation and composition deviation amplitudes for diffusivity ratio $D_A/D_B=100$. The inset shows the exact solution at very early stages. While the relaxation rates are sensitive to the ratio $D_A/D_B$, for a range of values $D_A/D_B=10-10^4$, we have found the extent of alloy decomposition to be nearly identical, the peak value of $\zeta_s$ lying between −0.05 and −0.065. For purposes of computation, all lengths are nondimensionalized by the length scale $L=\Omega\gamma/k_BT$ (such that $H=h/L$, $X=x/L$, etc.) and time is nondimensionalized as $\tau=(D_A\rho_s\Omega^2\gamma/k_BTL^4)\times t$.

To understand the roles of the two rates in surface relaxation, we solve Eq. (6) for the initial conditions $h(x,0)=h_0e^{ikx}$ and $\zeta_s(x,0)=0$, which correspond to a sinusoidal height modulation on the alloy surface with uniform surface composition $c_s=c_b$. The time-dependent height and composition amplitudes $h$ and $\zeta_s$, defined via $[h(x,t),\zeta_s(x,t)]\equiv[h(t),\zeta_s(t)]e^{ikx}$, are obtained as

$$h(t)=h_0\frac{(B_1k^4-\omega_2)e^{-\omega_1t}-(B_1k^4-\omega_1)e^{-\omega_2t}}{\omega_1-\omega_2}, \quad (11a)$$

$$\zeta_s(t)=-h_0\frac{(B_1k^4-\omega_1)(B_1k^4-\omega_2)}{A_1k^2(\omega_1-\omega_2)}(e^{-\omega_1t}-e^{-\omega_2t}). \quad (11b)$$

The relaxation behavior given by the above equations is plotted in Fig. 1 for a 50-50 alloy with $D_A/D_B=100$ and material parameters listed in Table I. The regimes of fast initial relaxation followed by slow long-time relaxation are clearly visible. In particular, the surface composition shows a rapid initial rise controlled by $\omega_1$ (given in the inset in Fig. 1), followed by a slowing down to attain an extremum as dictated by the competition between the two exponential terms in Eq. (11b), and a subsequent decay (controlled by $\omega_2$) asymptotically to zero. While the exact analytical expression for the extremum of $\zeta_s(t)$, denoted by $\zeta_s^*$, may be computed from Eq. (11b), it is of particular interest to note that

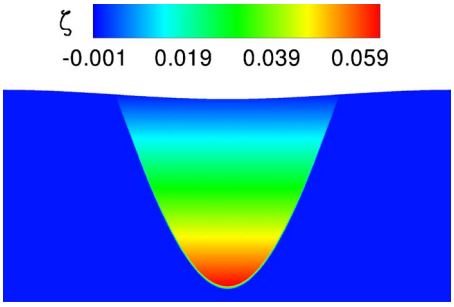


FIG. 2. (Color online) Vertical compositional gradients for an almost fully relaxed sinusoidal modulation with $D_A/D_B=100$. The enrichment in the $A$ species at the bottom of the "valley" occurs due to rapid diffusion of fast-moving $A$ atoms at initial times, controlled by $\omega_1$ (see discussion in the text). After attaining a maximum in the $A$ species, the composition returns exponentially to the equilibrium value as the profile flattens. (The surface layer of thickness $\delta_s$ is not shown.)

$$\zeta_s^* = -h_0 \frac{\Omega\gamma}{k_B T} \frac{c_b(1-c_b)(D_A-D_B)}{D_A(1-c_b)+D_B c_b} k^2 + O(k^4), \qquad (12)$$

which implies that the maximum extent of alloy segregation is, to leading order, inversely proportional to the *square* of the modulation wavelength. Also note that the overall relaxation rate $\omega_2$ is inversely proportional to the *fourth* power of the wavelength. From these two observations, it is clear that the modulation wavelength must be small (nanoscale) both for relaxation to be observable over realistic times as well as for significant alloy decomposition to occur.

This relaxation behavior observed in Fig. 1 may be understood as follows. At initial times, capillary effects cause rapid diffusion of species $A$ from the peaks of the modulation to the valleys at a rate determined by $\omega_1$, leading to alloy decomposition. However, since there is no energetic tendency for the alloy to phase separate (within the context of this work), compositional gradients seek to rectify this decomposition, thereby leading to the slowing down of $\zeta_s(t)$. At the extremum of $\zeta_s(t)$, capillary and compositional driving forces exactly balance each other and thereafter, the restoring force drives the composition asymptotically to equilibrium at a rate $\omega_2$ and the profile inexorably flattens. The lateral and temporal variations in surface composition also lead to vertical composition gradients in the valleys of the modulation, which persist indefinitely in the absence of bulk diffusion as each surface layer is overlaid in the valley by a new layer of different composition. An example of such vertical gradients, calculated for the same parameters as before, is illustrated in Fig. 2.

The physical meaning of the relaxation rate $\omega_2$ that in effect determines surface relaxation can be better understood by taking the limit $D_B \ll D_A$, where the diffusion of the $B$ species is very slow. In this limit, since $D_2^{\text{eff}}=D_B/(1-c_b)$, relaxation is completely controlled by the slower species $B$. Note, however, that the effective diffusivity is not merely the diffusivity of species $B$ but is enhanced by a factor of $(1-c_b)^{-1}$. This is because the fast diffusing species fills up most of the sites corresponding to its bulk stoichiometry $c_b$, as it diffuses from the peaks to the valleys, thereby leaving only a fraction $1-c_b$ of total sites to be filled by the slower species.

Based on numerical studies, Tersoff [5] noted the existence of two distinct regimes of exponential decay for the relaxation of a modulation on a two-component surface. However, his results were restricted to the very early stages of evolution (specifically, ~0.5% decay in amplitude of a sinusoid), which is entirely within the regime of initial transients identified in our work. Consequently, he did not provide an estimate for the long-time relaxation rate, nor was the turnover in composition evolution clearly identified. In contrast, our analytical results provide a complete description with precise scaling estimates for relaxation.

## IV. RELAXATION BY SURFACE AND BULK DIFFUSION

Next, we consider the more general case where both surface and bulk diffusion are operative ($D_b \neq 0$). It is convenient to report our results in terms of a dimensionless parameter $R_b=D_b L/D_A \rho_s \Omega$ that determines the relative contributions to mass transport from surface and bulk diffusion. To see this more clearly, note that $D_A\rho_s = (D_0/a^2)e^{-(E_d+E_f)/k_BT} \equiv D_{A,s}/a^2$, where $D_0$ is an Arrhenius prefactor, $E_d$ is the energy barrier for surface diffusion, $E_f$ is the adspecies formation energy, and $a^2$ is the surface area associated with the adspecies [8]. With these definitions, $R_b = (D_b/D_{A,s}) \times (\text{La}^2/\Omega)$. The factor $\text{La}^2/\Omega$ is material specific, but roughly estimated to be 1. Thus $R_b \approx D_b/D_{A,s}$ is a direct measure of the relative importance of bulk and surface diffusion. Qualitatively, bulk diffusion will smooth out composition gradients at the surface induced by differences in the surface diffusivities of the alloy components, thereby reducing the extent of kinetic surface segregation. Furthermore, since countering alloy decomposition involves the exchange of atoms of the slower species that accumulate at the peaks with atoms of the faster species from the bulk, the overall flattening of the profile is sped up. These and other features are discussed in quantitative detail below.

We seek to solve the surface evolution equations (6a) and (6b) in conjunction with the bulk diffusion equation (6c). The coupling between surface and bulk diffusion occurs in two ways: first, there is a direct coupling via the last term in Eq. (6b) that accounts for interdiffusion between the surface layer and the bulk, and second, there is an indirect coupling wherein the surface composition at any given instant provides one of the two requisite boundary conditions for the bulk diffusion equation as explained below. If the solution to the bulk diffusion equation is known, the last term in Eq. (6b) can be readily evaluated and the problem reduced to solving only Eqs. (6a) and (6b). Since the equations are all linear, the bulk field must have the same Fourier representation as the surface fields in the lateral ($x$) direction and may be written as $\zeta(x,y,t)=\bar{\zeta}(y,t)e^{ikx}$—note that the amplitude of the composition modulation must be allowed to vary with distance from the surface layer ($y$ direction). As before, the initial condition is taken to be one of uniform composition $\zeta(x,y,0)=0$. Since we do not consider alloy segregation or

nonequilibrium surface fluxes [7], as noted in Sec. I, the surface composition $\zeta_s(x,t)$ is equal to the limiting value of the bulk composition $\zeta(x,0,t)$ at the bulk-surface interface—this requirement provides one boundary condition. The other boundary condition is provided by $\zeta(x,-\infty,t)=0$, which ensures that compositional variations decay to zero at $-\infty$ at all times.

To summarize the above discussion, we first solve

$$\frac{\partial \zeta}{\partial t} = D_b\left(\frac{\partial^2}{\partial x^2} + \frac{\partial^2}{\partial y^2}\right)\zeta, \tag{13}$$

in the domain $-\infty < x < \infty, -\infty < y \leqslant 0$ with initial and boundary conditions

$$\zeta(x,y,0) = 0, \quad \zeta(x,0,t) = \zeta_s(x,t), \quad \zeta(x,-\infty,t) = 0. \tag{14}$$

The amplitude $\bar{\zeta}(y,t)$ of the bulk composition modulation, defined via $\zeta(x,y,t)=\bar{\zeta}(y,t)e^{ikx}$, can now be obtained using integral transform methods as

$$\bar{\zeta}(y,t) = -\frac{y}{2\sqrt{\pi D_b}}\int_0^t \zeta_s(t')\frac{e^{-k^2 D_b(t-t')}e^{-[y^2/4D_b(t-t')]}}{(t-t')^{3/2}}dt'. \tag{15}$$

Note that the result obtained is nonlocal in time and depends upon the entire history of compositional variations at the surface. In principle, the solution for the bulk field may now be used to determine the last term in Eq. (6b) and convert it to an integrodifferential equation that is nonlocal in time. However, the resulting surface diffusion equations that must then be solved are intractable and so we choose to work instead in Laplace transformed variables. By using Eq. (15), the Laplace transform [22] of the bulk field is obtained as

$$\tilde{\zeta}(x,y,p) = \tilde{\zeta}_s(p)e^{\sqrt{(p/D_b)+k^2}y}e^{ikx}, \tag{16}$$

which may now be used in Eq. (6b) to obtain a set of algebraic equations for the height and surface composition amplitudes (in transformed variables) as

$$p\tilde{H}(p) = H_0 - A_1\tilde{\zeta}_s(p) - B_1\tilde{H}(p), \tag{17a}$$

$$p\tilde{\zeta}_s(p) = -A_2\tilde{\zeta}_s(p) - B_2\tilde{H}(p) - \frac{D_b}{\delta_s}\sqrt{\frac{p}{D_b}+k^2}\tilde{\zeta}_s(p). \tag{17b}$$

These equations are readily solved for $\tilde{H}(p)$ and $\tilde{\zeta}_s(p)$ to obtain the height of the modulation as well as the surface composition in transformed variables. While we are unable to invert these transforms analytically to obtain solutions in physical variables, they are amenable to numerical inversion using standard routines [9] available in MATHEMATICA.

A parametric study of ripple evolution in the presence of bulk diffusion is presented in Fig. 3. Alloy decomposition caused by capillary effects is now compensated by both surface and bulk diffusion. When the contribution from bulk diffusion is negligible ($R_b \to 0$), the effective diffusivity for long-time relaxation [Eq. (10b)]

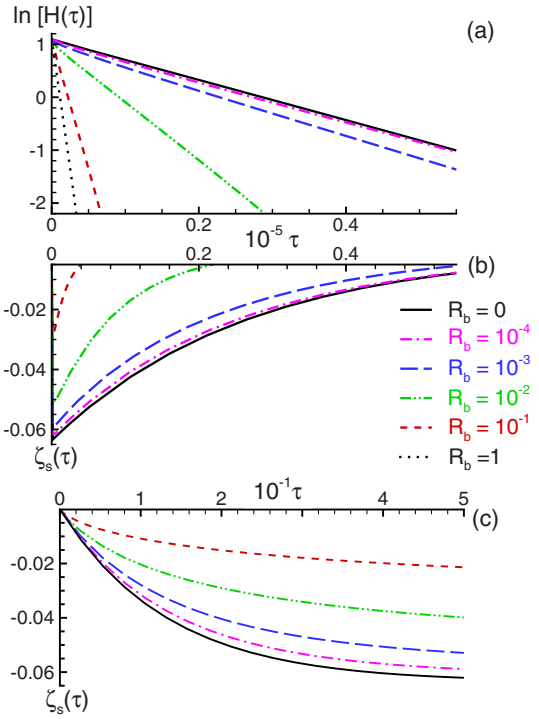


FIG. 3. (Color online) Evolution of (a) height and [(b) and (c)] composition deviation amplitudes as a function of the dimensionless parameter $R_b$ that measures the relative importance of bulk and surface diffusion (see the text). The ratio of surface diffusivities $D_A/D_B=100$ in these calculations. For a range of values $D_A/D_B=10-10^4$, we find that bulk diffusion typically becomes significant when $R_b=10^{-2}-10^{-3}$. The initial stages of relaxation, where bulk diffusion plays a more prominent role in compensating for surface alloy decomposition, are shown in (c). For purposes of computation, all lengths are nondimensionalized by the length scale $L=\Omega\gamma/k_BT$ and time is nondimensionalized as $\tau=(D_A\rho_s\Omega^2\gamma/k_BTL^4)\times t$.

$$D_2^{\text{eff}} = \frac{D_A D_B}{D_A(1-c_b)+D_B c_b}$$

is determined as before by the slower diffusing species. However, when bulk and surface contributions are comparable ($R_b$ close to 1), bulk diffusion is seen to be very effective in compensating the alloy decomposition brought about by surface diffusion. The composition term in Eq. (6a) is negligible in this limit and the modulation decays with an effective diffusivity

$$D_b^{\text{eff}} = D_A c_b + D_B(1-c_b), \tag{18}$$

which is the *composition-weighted* average of the diffusivities of the two species. The ratio of the corresponding relaxation rates ($\omega_b$ denoting the rate for combined surface and bulk diffusion) is

$$\frac{\omega_b}{\omega_2} = \frac{D_b^{\text{eff}}}{D_2^{\text{eff}}} \propto \frac{D_A}{D_B}. \tag{19}$$

The difference in relaxation rates is clearly significant when species $A$ is much faster than species $B$. For intermediate

values of $R_b$, bulk diffusion plays a role in smoothing out sharp composition gradients that primarily occur at initial times. Indeed, from Fig. 3, increasing values of $R_b$ are clearly seen to suppress the maximum extent of kinetic segregation at the surface. Irrespective of the magnitude of $R_b$, the *overall* relaxation is still dominated by surface diffusion, which can be readily verified by comparing the magnitudes of the first and last terms (surface vs bulk contributions) in Eq. (17b).

## V. IMPLICATIONS OF INTERDIFFUSION FOR SURFACE RELAXATION

The results presented in the previous section indicate that bulk diffusion affects surface relaxation only when $R_b > 10^{-3}$—it is therefore worthwhile to examine the implications for practical cases. As an example, for SiGe films a typical value of $D_{A,s}$ at 600 °C is $10^{-10}$–$10^{-11}$ $cm^2/s$ [10–12]. Interdiffusion coefficients in SiGe films are reported to be as low as $10^{-18}$–$10^{-19}$ $cm^2/s$ [13,14] at 770–870 °C or, alternatively, as high as $10^{-10}$–$10^{-13}$ $cm^2/s$ at 600–900 °C [15]. The first range of values suggests that $R_b$ is so small that bulk diffusion is entirely insignificant [16] whereas the second range of values would suggest that bulk diffusion can indeed exert an influence on alloy decomposition and intermixing during heteroepitaxial growth. Indeed, if the latter case is borne out, interdiffusion would play a particularly important role in the growth of the wetting layer (very initial stages) for Stranski-Krastanov growth of $Si_{1-x}Ge_x$/Si or Ge/Si films. In other situations where surface diffusion is suppressed by surfactants such as As, Sb, C [17–19], intermixing via bulk diffusion will play a more prominent role in surface evolution—an analysis that accounts for both bulk and surface diffusion, as in this work, then becomes essential. Our results that combine surface and bulk diffusion could also be of relevance in metal silicides where rapid bulk diffusion pathways for metal atoms have been observed [20]. Recent phase-field calculations [21] of thermal grooving in polycrystalline Ni-Si thin films with slow-diffusing Pt impurities also demonstrate the importance of bulk diffusion *perpendicular* to grain boundaries in setting the agglomeration time. Our analysis, with appropriate modifications, could then be extended to the evolution of interfaces between alloy grains.

## VI. CONCLUDING REMARKS

To summarize, we have presented a model for relaxation of alloy surfaces that accounts for the effects of both surface and bulk diffusion. In the limit of negligible bulk diffusion, we have provided exact analytical expressions for relaxation rates that can be used to interpret experiments and extract diffusion constants in two component systems. When bulk diffusion is within a couple of orders of magnitude of surface diffusion, intermixing has been shown to play a role in reducing alloy segregation as well as accelerating the overall relaxation rate. While the work here has been restricted to isotropic surfaces, it is readily extended to singular and vicinal surfaces of crystals and will be reported elsewhere.

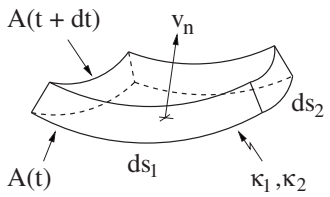


FIG. 4. Evolution of a differential element of area $A$ at the film surface. The lengths of the edges of the element measured in the local coordinate system $(s_1, s_2)$ are $ds_1$ and $ds_2$. The normal velocity of the element is $v_n$. The principal curvatures are $\kappa_1$ and $\kappa_2$ (positive for concave-up surface).

## ACKNOWLEDGMENT

The research support of the USDOE under contract DE-FG02–01ER45913 is gratefully acknowledged.

## APPENDIX A: DERIVATION OF SURFACE EVOLUTION EQUATIONS

The derivation of Eqs. (2) and (4) is briefly noted here. A more general treatment for an interface between two phases may be found in Appendix A of Ref. [6].

Consider the evolution during an infinitesimal interval of time $dt$ of a differential element of area $A$ with principal curvatures $\kappa_1$ and $\kappa_2$ at the solid-vacuum interface (Fig. 4). The surface is parametrized by a local coordinate system $(s_1, s_2)$, $ds_1$ and $ds_2$ denoting the lengths of the edges of the differential element. The element moves normal to itself with velocity $v_n$. Let $n_{s,i}$ and $n_{v,i}$ denote the number density of species $i$ at the surface and in the bulk, respectively. The total number of particles of species $i$ contained in the differential element at time $t$ is $n_{s,i}(t)A(t)$ while that at time $t+dt$ is $n_{s,i}(t+dt)A(t+dt)$, the net change in the number of particles being

$$\begin{aligned} & n_{s,i}(t+dt)A(t+dt) - n_{s,i}(t)A(t) \\ & \quad \approx \left( \frac{\partial n_{s,i}}{\partial t} A(t) + \frac{\partial A}{\partial t} n_{s,i}(t) \right) dt \\ & \quad = \left( \frac{\partial n_{s,i}}{\partial t} - v_n n_{s,i} \kappa \right) A(t) dt, \end{aligned} \tag{A1}$$

where $\kappa = \kappa_1 + \kappa_2$ is the sum of the principal curvatures. The surface fluxes $j_i(s_1, s_2)$ lead to a net accumulation of particles in the differential element given by

$$\begin{aligned} & [j_i(s_1, s_2, t) - j_i(s_1 + ds_1, s_2, t)] ds_2 dt \\ & \quad + [j_i(s_1, s_2, t) - j_i(s_1, s_2, + ds_2, t)] ds_1 dt \\ & \quad = - \left( \frac{\partial j_i}{\partial s_1} + \frac{\partial j_i}{\partial s_2} \right) ds_1 ds_2 dt \\ & \quad = - \nabla_s \cdot \mathbf{j}_i A(t) dt. \end{aligned} \tag{A2}$$

Finally, as the surface advances normal to itself it loses particles to the bulk whereas if it recedes normal to itself it gains particles from the bulk. The net accumulation of particles is thus given by

$$- n_{v,i} v_n A(t) dt. \tag{A3}$$

Conservation of particles then demands that

$$\left( \frac{\partial n_{s,i}}{\partial t} - v_n n_{s,i} \kappa \right) = - \nabla_s \cdot \mathbf{j}_i - n_{v,i} v_n. \tag{A4}$$

If we assume that there is no surface segregation, the surface composition is merely the limiting value of the bulk composition at the surface. The areal number density at the surface is then proportional to the volume number density and may be expressed as $n_{s,i} = \delta_s n_{v,i}$, where $\delta_s$, which has dimensions of length, may be interpreted as an interface width. Further, the volume number density is related to the bulk composition as $n_{v,i} = c_{\Gamma,i}/\Omega$, $\Omega$ being the atomic volume, which is assumed for convenience to be the same for both species. The bulk composition of species $i$, denoted by $c_{\Gamma,i}$, is the composition of the material immediately below the surface. For the case of relaxation, in regions where the surface recedes locally (material depletion) $c_{\Gamma,i}$ is the composition of the subsurface bulk whereas in regions where the surface advances locally (material accumulation) $c_{\Gamma,i}$ is the instantaneous composition of the surface itself. In the presence of a deposition flux, $c_{\Gamma,i}$ is the instantaneous composition of the surface since material at the surface is overlaid by the arriving flux of atoms thereby becoming the subsurface at the next instant. In the case of ion erosion [7], $c_{\Gamma,i}$ is always the bulk composition since the incident ion beam sputters away the surface layer and continuously exposes the underlying bulk. Noting further that $n_{s,i} = \delta_s c_{s,i}/\Omega$, the conservation equations (A4) may be rewritten as

$$\delta_s \frac{\partial c_{s,A}}{\partial t} = - \Omega \nabla_s \cdot \mathbf{j}_A - c_{\Gamma,A} v_n (1 - \delta_s \kappa),$$

$$\delta_s \frac{\partial c_{s,B}}{\partial t} = - \Omega \nabla_s \cdot \mathbf{j}_B - c_{\Gamma,B} v_n (1 - \delta_s \kappa). \tag{A5}$$

In the limit of negligible vacancy concentration at the surface, $c_{s,A} + c_{s,B} = 1$ and the preceding equations may then be combined into a single one, namely, Eq. (4), as

$$\delta_s \frac{\partial c_s}{\partial t} = \Omega [(c_\Gamma - 1) \nabla_s \cdot \mathbf{j}_A + c_\Gamma \nabla_s \cdot \mathbf{j}_B], \tag{A6}$$

where $c_s \equiv c_{s,A}$ and $c_\Gamma = c_{\Gamma,A}$. We note from this result that the change in surface composition $c_s$ is driven purely by deviations of the ratio of mass fluxes $\nabla_s \cdot \mathbf{j}_A / \nabla_s \cdot \mathbf{j}_B$ from the ratio $c_\Gamma/(1 - c_\Gamma)$. Also, adding the two equations (A5), and invoking the approximation $\delta_s \kappa \ll 1$, which holds if the interface width is much smaller than the profile wavelength, we obtain Eq. (2).

## APPENDIX B: DERIVATION OF LINEARIZED GOVERNING EQUATIONS

We outline the essential steps in deriving the linearized evolution equations (6) from the nonlinear governing equations (1), (2), (4), and (5) of the model.

For the case of one-dimensional surface perturbations, which is the situation of interest here, the governing equations may be written in a simpler form as follows:

$$j_i = - D_i \rho_s \frac{\partial c_{s,i}}{\partial s} + \frac{D_i c_{s,i} \rho_s \Omega \gamma}{k_B T} \frac{\partial \kappa}{\partial s}, \tag{B1a}$$

$$v_n = - \Omega \frac{\partial}{\partial s} (j_A + j_B), \tag{B1b}$$

$$\delta_s \frac{\partial c_s}{\partial t} = \Omega \left[ (c_\Gamma - 1) \frac{\partial j_A}{\partial s} + c_\Gamma \frac{\partial j_B}{\partial s} \right] - D_b \left. \frac{\partial c}{\partial n} \right|_\Gamma, \tag{B1c}$$

$$\frac{\partial c}{\partial t} = D_b \left( \frac{\partial^2}{\partial x^2} + \frac{\partial^2}{\partial y^2} \right) c. \tag{B1d}$$

Now consider the evolution of small perturbations in height and composition, i.e., $|\nabla_s h| \ll 1$ and $(c - c_b) \equiv \zeta \ll 1$, respectively. First, we parametrize the height $h$ of the film surface by the $x$ coordinate, i.e., $h \equiv h(x,t)$, rather than the arclength $s$; this representation is valid even for large slopes as long as $h$ is single valued (no surface overhangs). Next, in the small-slope limit, the following approximations hold: (1) $\partial/\partial s \approx \partial/\partial x$, (2) the normal velocity of the surface $v_n \equiv (\partial h/\partial t)/\sqrt{1 + (\partial h/\partial x)^2} \approx \partial h/\partial t$, and (3) the surface curvature $\kappa \approx \partial^2 h/\partial x^2$. Also note that in terms of our new variable $\zeta$, $c_{s,A} = c_b + \zeta_s$, $c_{s,B} = 1 - c_b - \zeta_s$, and $c = c_b + \zeta$; $\zeta_s$ itself is the limiting value of the bulk field $\zeta$ at the surface, which is a valid statement as long as there is no surface segregation. For convenience, we assume that the film-substrate interface $\Gamma$, rather than the film surface itself, is located at $y = 0$. Making the necessary substitutions in Eq. (B1a) and retaining only the lowest order terms in $h$ and $\zeta$, we have

$$j_A = - D_A \rho_s \frac{\partial \zeta_s}{\partial x} + \frac{D_A c_b \rho_s \Omega \gamma}{k_B T} \frac{\partial^3 h}{\partial x^3},$$

$$j_B = D_B \rho_s \frac{\partial \zeta_s}{\partial x} + \frac{D_B (1 - c_b) \rho_s \Omega \gamma}{k_B T} \frac{\partial^3 h}{\partial x^3}. \tag{B2}$$

Substituting these fluxes in Eqs. (B1b)–(B1d), keeping in mind the approximations listed above, we readily obtain the linearized equations (6).

[1] C. Herring, in *Structure and Properties of Solid Surfaces*, edited by R. Gomer and C. S. Smith (University of Chicago Press, Chicago, 1953), p. 5.
[2] W. W. Mullins, J. Appl. Phys. **28**, 333 (1957); **30**, 77 (1959).
[3] J. M. Blakely and H. Mykura, Acta Metall. **10**, 565 (1962).
[4] P. S. Maiya and J. M. Blakely, J. Appl. Phys. **38**, 698 (1967).
[5] J. Tersoff, Appl. Phys. Lett. **83**, 353 (2003).
[6] B. J. Spencer, P. W. Voorhees, and J. Tersoff, Phys. Rev. B **64**,

235318 (2001).
[7] V. B. Shenoy, W. L. Chan, and E. Chason, Phys. Rev. Lett. **98**, 256101 (2007).
[8] A. Pimpinelli and J. Villain, *Physics of Crystal Growth* (Cambridge University Press, Cambridge, England, 1998).
[9] A. Mallet, *Numerical Inversion of Laplace Transform*, URL http://library.wolfram.com/infocenter/MathSource/2691/
[10] N. C. Bartelt, W. Theis, and R. M. Tromp, Phys. Rev. B **54**, 11741 (1996).
[11] T. Schwarz-Selinger, Y. L. Foo, D. G. Cahill, and J. E. Greene, Phys. Rev. B **65**, 125317 (2002).
[12] F. Watanabe, D. G. Cahill, and J. E. Greene, Phys. Rev. Lett. **94**, 066101 (2005).
[13] D. B. Aubertine, N. Ozguven, and P. C. McIntyre, J. Appl. Phys. **94**, 1557 (2003).
[14] D. B. Aubertine and P. C. McIntyre, J. Appl. Phys. **97**, 013531 (2005).
[15] S. Zheng, M. Kawashima, M. Mori, T. Tambo, and C. Tatsuyama, Thin Solid Films **508**, 156 (2006).
[16] N. Motta, F. Boscherini, A. Sgarlata, A. Balzarotti, G. Capellini, F. Ratto, and F. Rosei, Phys. Rev. B **75**, 035337 (2007).
[17] R. M. Tromp and M. C. Reuter, Phys. Rev. Lett. **68**, 954 (1992).
[18] B. Voigtländer, A. Zinner, T. Weber, and H. P. Bonzel, Phys. Rev. B **51**, 7583 (1995).
[19] A. Bernardi, J. O. Ossó, M. I. Alonso, A. R. Goñi, and M. Garriga, Nanotechnology **17**, 2602 (2006).
[20] M. Y. Lee and P. A. Bennett, Phys. Rev. Lett. **75**, 4460 (1995).
[21] M. Bouville, D. Chi, and D. J. Srolovitz, Phys. Rev. Lett. **98**, 085503 (2007).
[22] The Laplace transform is defined as $\mathcal{L}[f(t)] \equiv \tilde{f}(p) = \int_0^\infty e^{-pt} f(t) dt$.